Summer 8-11-2015

Study of Piezo-phototronic Effect on Type-II Heterojunction ZnO/ZnSe Core/Shell Nanowire Array

Fahad Alqarni
Fahad-119@hotmail.com

Fahad Dhafer Alqarni
falqarni@uno.edu

Study of Piezo-phototronic Effect on Type-II Heterojunction ZnO/ZnSe Core/Shell Nanowire Array

A Thesis

Submitted to the Graduate Faculty of the
University of New Orleans
in partial fulfillment of the
requirements for the degree of

Master of science
Chemistry

by
Fahad Alqarni
B.S. University of Tabuk, 2011
August, 2015

Acknowledgments

I would like to express my deepest gratitude to my advisor, Prof. Weilie Zhou, for his continued support and guidance throughout my M.S. study. His enthusiasm to work and patience with students has greatly impressed me. I gratefully thank the academic committee members: Prof. Mark Trudell and Prof. John Wiley for their valuable discussion, insightful suggestions and constructive comments during my study and research. I would also like to thank my research group members Nooraldeen Alkurd, Manish Bhatt, Amaury Menard, Satish Rai, Michael Retana, Sarah Wozny, Shuke Yan and Zhi Zheng for their help during my stay. Finally, a special thanks and appreciation goes out to my family for their support, encouragement and patience during my study.

Table of Contents

List of Figures

List of Tables

Abstract

A two-step synthesis was performed to fabricate type-II heterojunction ZnO/ZnSe core/shell nanowires. First, ZnO core NWs were synthesized on ITO substrate via chemical vapor deposition (CVD). Then pulsed laser deposition (PLD) technique was carried out to coat the ZnO core with ZnSe Shell. The ZnO/ZnSe core-shell NWs which has application on optoelectronics, such as photodetectors and photosensors were characterized via scanning electron microscope (SEM), transmission electron microscope (TEM) and finally photodetector devices were measured via current–voltage characteristics under ultraviolet (UV) illumination to investigate the effect of the inner piezopotential. The ZnO-nanowire-based photodetector ultraviolet (UV) light devices with core/shell structure show excellent photo-responsivities. Ultimately, the results in this work of ZnO/ZnSe core/shell heterojunction with excellent piezoelectric properties is demonstrated to show great promise in the piezo-phototronic device application.

Keywords: Photodetectors; Piezo-phototronic effect; Core/shell nanowires; Epitaxial growth; Type-II heterojunction

Introduction and Background

Recent development advances have allowed wide band-gap II-VI compound semiconductors to approach applications of these materials to fabricate novel devices, such as optoelectronic devices, light emitting diode, laser diode, solar cell, sensor, pyroeletric & piezoelectric devices, self-compensating gas sensor, substrate transparent electrode, electronic devices, filed-effect transistor, high power electronic devices, low threshold optical pumping, SAW devices, SAW filter and SAW oscillator. Wide band-gap II-VI compound semiconductors can be obtained when group II elements and group VI elements are combined in a synthetic way. In addition, wide-bandgap II–VI compounds such as ZnS, ZnO, ZnSe, ZnTe, CdSe and CdTe have been studied and applied to optoelectronic devices like photodetectors or photosensors (1).

We begin with a study of some of the properties of zinc oxide (ZnO) and zinc selenide (ZnSe) semiconductor materials. The reason for the higher melting point for zinc oxide (ZnO) and zinc selenide (ZnSe) is due to the high ionicity of wide-bandgap II–VI compounds. Also, the nature of direct and wide-band gap zinc oxide (ZnO) and zinc selenide (ZnSe) semiconductors allow them to be ultraviolet (UV) and visible to light detection. The advantage of utilizing wide bandgap semiconductor such as ZnSe with ZnO to form type-II heterostructures to generate narrower indirect bandgap will improve the charge carrier collection which leads to reduced recombination losses. Thus, synergistic effect between the two components ZnO/ZnSe and abrupt interfacial potential between the core and shell materials allow photodetector devices to detect photons with energies significantly smaller than~2.2 eV (2). The structure of type II heterojunction ZnO/ZnSe core/shell nanowire array is schematically illustrated in Figure 1.1. The fact is that a core/shell structure has been utilized to fabricate the photodetector devices due to its favorable radial geometry, which can improve the charge carrier collection and reduce recombination losses (3).

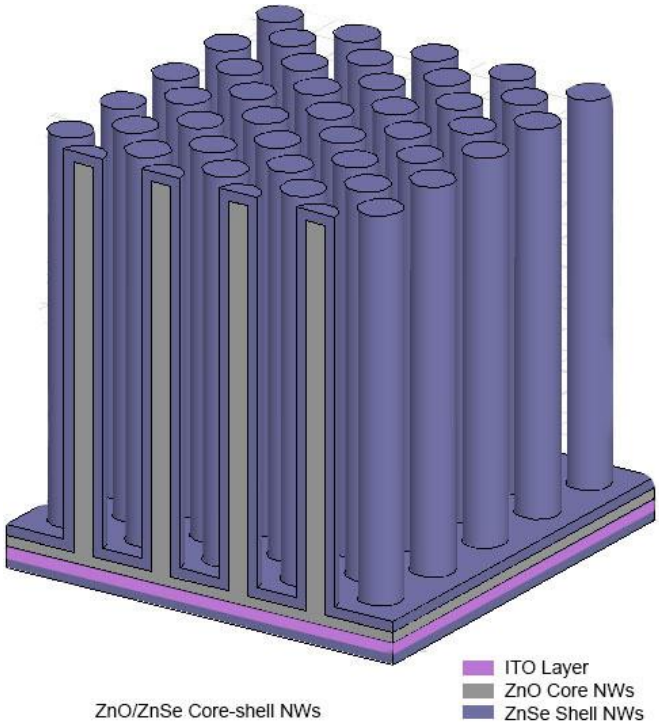

Figure 1.1 Schematic representation of type II heterojunction ZnO/ZnSe core/shell nanowire array

1.1 The basics of ZnO

Zinc oxide (ZnO) is a II-VI compound semiconductor, which is called a multifunctional material due to its unique physical and chemical properties. Zinc oxide is an intrinsic n-type semiconductor because of a deviation from stoichiometry, due to the presence of intrinsic defects such as oxygen vacancies and zinc interstitials (4). Its application for optoelectronics refers to its physical and chemical properties, such as high chemical stability, high electrochemical coupling coefficient, broad range of radiation absorption and high photostability (5).

Zinc oxide is an attractive semiconductor material that displays semiconducting and piezoelectric properties. It has been studied and found to be a very promising material for optoelectronic devices. The wide range of useful properties, including high electron mobility 100 cm^2/Vs, high thermal conductivity, large exciton binding energy ~60meV (electron-hole binding energy) and high thermal and mechanical stability, making it suitable for optoelectronic devices (6) and (7).

Additionally, zinc oxide mainly exhibits a wide and direct bandgap ~3.37 eV. Since the zinc oxide (ZnO) bandgap is too large for visible light absorption, it makes it very attractive for optoelectronic devices in the near UV region. Besides, the inherent piezoelectric property of ZnO can produce voltage output from applied stress. Therefore, the semiconducting and piezoelectric properties of ZnO means that it can be used as photodetectors (8).

Zinc oxide (ZnO) which is an important and promising metal oxide has been widely studied in many areas because of its diverse properties and potential applications. ZnO as a semiconductor has been used for medicinal purposes and in electronics, such as in laser diodes, LED's, transparent thin film coatings, and various piezoelectrics. Practically, it shows very promising application in nanoscale range, such as ultralight UV detectors, actuators, transistors, sensors, etc (9).

Physical parameters of ZnO	
Physical parameters	Values
bandgap energy Eg	3.37 eV
space group	$P6_3mc$
a	0.32495 nm
c	0.52069 nm
Crystal structure	Wurtzite
Density	5.606 g cm^{-3}
Melting point	1975 °C
Exciton binding energy	60 meV
Electron affinity	4.3 eV

Table 1.1 Typical physical parameters of zinc oxide (ZnO) (10) & (11).

1.1 The basics of ZnSe

Zinc selenide (ZnSe), a II-VI compound semiconductor with cubic zinc blende structure and a direct bandgap of 2.7 eV, is considered a very favorable semiconductor material for optoelectronic devices. Due to its great bandgap as well, it has low optical absorption in the visible and infrared spectral region. It has potential to be used in optoelectronic devices such as light emitting diodes, optical coatings, ultrasonic transducers, and photodetectors due to its wide range of useful properties, such as large band gap, low resistivity and photosensitivity (12).

Physical parameters of ZnSe	
Physical parameters	Values
bandgap energy Eg	2.7 eV
space group	$F\bar{4}3m$
a	0.567 nm
Crystal structure	Zincblende (cubic)
Density	5.27 g cm^{-3}
Melting point	1525 °C
Exciton binding energy	20 meV
Electron affinity	4.09 eV

Table 1.2 Typical physical parameters of zinc selenide (ZnSe) (10) & (13).

1.2 Importance of piezo electronic materials

Piezoelectric materials are semiconductor compounds and possess a wurtzite structure that has been used since the beginning of the 18th century. Piezo is a Greek word which means to squeeze or press, while piezoelectric means electricity resulting from pressure (14). There are two types of piezoelectric materials, which are natural or synthetic. The natural piezoelectric materials, such as Quartz, Tourmaline and Rochelle, and some of the most used synthetic piezoelectric materials nowadays, such as ZnO, GaN, InN, and CdS, shows electric, semiconducting and photoexcitation

properties (15). These piezoelectric materials have been employed in an impressive range of applications, such as piezoelectric resonators, transducers, sound emitters, receivers, solar cells, photodetectors and LEDs. Moreover, sonar is a sound navigation and ranging, which is a device used for board ships, boats and submarines to detect other sonar objects under water. TMD is a tuned mass damper device that is used in skyscrapers at the top of the building as a motion control device. TMD is a system being used in skyscrapers to stabilize the building in the case that its stability is ever threaten by earthquakes, storms, or heavy winds (16). Therefore, piezoelectric materials are very important in our lifestyle and in the following paragraphs the coupling system, important definitions, effects and mechanism of these materials will be discussed.

Piezoelectric potential or piezopotential is created when pressure/stress is applied upon the piezoelectric material. For instance, there are several ways that the coupling system can be combined and therefore each coupling system or sometimes combination of them can be used for a variety of applications of the piezoelectric material, such as Piezotronics, Piezophotonics, Opto-electronics and Piezo phototronics. *Piezotronics* can be obtained when piezo-electricity and semiconductor are coupled, while by joining piezo-electricity and photonic excitation, a *Piezophotonics* can be attained. Also, by coupling the semiconductor and photonic excitation, a *Piezo phototronics* can be achieved. Finally *Piezo-phototronics* is a result of the three-way-coupling between piezo-electricity, photonic excitation and semiconductor. Consequently, by using piezoelectric semiconductor materials, the piezoelectric, photoexcitation and semiconducting properties can be coupled together to investigate their physics and novel applications (17).

The elements ZnO, GaN, InN, and CdS in group II-VI and III-V in the periodic table are wide bandgap semiconductor materials that possesses piezopotential, which in turn leads them to be fabricated as a device causing their piezoelectric potential to be used. The piezopotential is an inner potential inside the crystal that is formed by non-mobile, non-annihilative ionic charges. There are two ways to study the piezopotential distribution inside nanowire. The first one is when an axial strain is introduced to the nanowire and the other is when a transverse strain is applied. In a theoretical study of piezoelectric field, using lattice-mismatched nanowire heterostructures can

significantly boost piezopotential inside the nanowire and this in turn improves charge carrier transport (18) and (19).

Recently, rapid progress in the dominant fields of piezo-phototronics and piezotronics has been observed. The significance of the *piezo-phototronic* devices are to use the inherent piezoelectric polarization to tune the charge generation, separation, and transport and/or recombination process at the interface for enhancing optoelectronic processes, while *piezotronics* is about using the built-in piezopotential as a 'gate' voltage to adjust charge-carrier transport across the metal–semiconductor contact or the p–n junction. Piezoelectric charges at the interface/junction can significantly affect the charge carrier separation and transport. For instance, when optoelectronic devices are fabricated using piezo-phototronic effect, their performance and interaction with light are significantly changed by externally applied strain. Finally, charge generation, separation, transport and recombination process are the essential physics of piezotronic and piezo-phototronics devices (20).

As it is very well known, piezoelectric materials can be used to convert mechanical energy into electric energy and vice versa. For instance, when an external voltage is applied to devices fabricated using the piezoelectric potential like sensors and actuators, a mechanical action or geometric deformation occurs, and this phenomena is known as "Inverse Piezoelectric Effect". Also, when piezoelectric semiconductor materials are under externally applied forces, an electric filed "voltage" will be generated, and this phenomena is called "Direct Piezoelectric Effect" (17) and (20).

The piezopotential of piezoelectric materials can be affected by applying light illumination and/or external strain. For light illumination, the effect of piezopotential reduces with increasing illumination intensity. For straining, a piezoelectric potential can be created under different straining conditions including stretching, twisting, bending, axial and transverse compression, and their combination. Upon straining, piezopotential continuously moves from one side of the nanowire to the other. Making electron increases from one end to the other (17) and (20).

Growth of ZnO nanowire

2.1 Background

The growth techniques of ZnO are very important since they influence their structure and since there are a lot of techniques to synthesize ZnO NWs, the choice method to make ZnO NWs for optoelectronic device is a crucial step. Choosing the appropriate method allows one to take advantage of its useful properties. Zinc oxide naturally crystallizes in wurtzite structure. ZnO which has a melting point of 2248 K typically show three types of growth direction like $[2\bar{1}\bar{1}0]$, $[01\bar{1}0]$ or [0001] (21). ZnO single crystals and semiconductors II–VI compounds can be epitaxially grown in a variety of ways, such as the hydrothermal method, vapour liquid solid (VLS) (22), liquid-phase epitaxy (LPE) (23), hot-wall epitaxy (HWE) (24), metalorganic chemical vapor deposition (MOCVD) (25) or metalorganic phase epitaxy (MOVPE) (26), molecular-beam epitaxy (MBE) (27) and atomic-layer epitaxy (ALE) (28). Therefore, the method being used for growing ZnO NWs can contribute to its properties and by taking advantage of the morphologies will therefore effectively enable scientists to optimize optoelectronic devices.

2.2 ZnO nanowire array grown on ITO by CVD

Various techniques have been used to grow c-axis-oriented ZnO compound semiconductor material. Different ZnO nanostructures grown by the Chemical Vapour Deposition (CVD) method are being used to design and fabricate novel optoelectronic devices. For epitaxial growth, Chemical Vapour Deposition considers one of the most employed techniques to obtain NWs with desirable mechanical, electrical, magnetic, optical or chemical properties. In Chemical Vapour Deposition, growth rate can be determined by several parameter temperature, pressure, and composition and chemistry of the gas-phase. Moreover, thickness of deposited materials can be precisely controlled using Chemical Vapour Deposition (29). So far, mechanism of reactions occurring in the chamber are still not fully understood. Besides, reaction processes are considerably complex and involve a series of gas-phase and surface reactions (30). As shown in Figure 2.1, it illustrates mechanism reaction processes are considerably complex and involve a series of gas-phase and surface reactions.

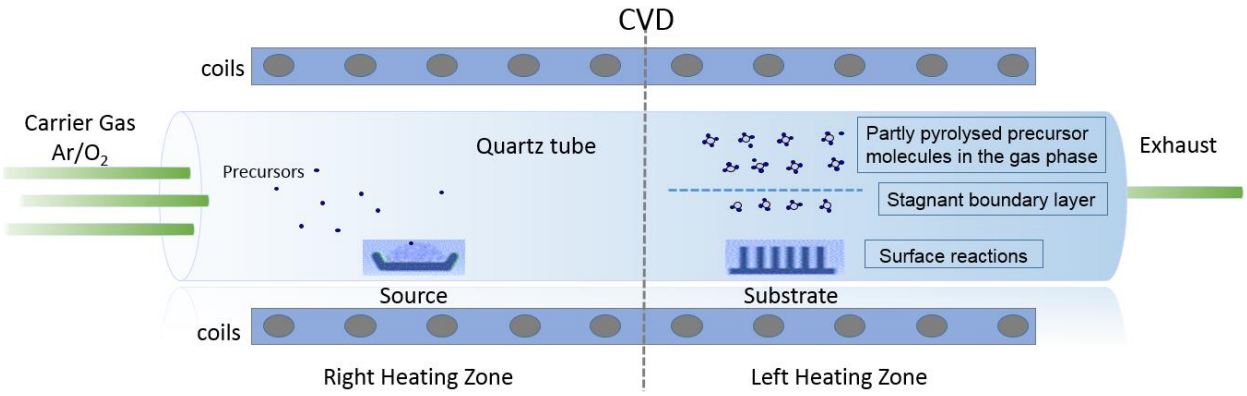

Figure 2.1 Schematic representation of the CVD Chemical Vapour Deposition process shows how ZnO NWs can be grown on ITO Substrate.

Synthesis

The ZnO powder was loaded into an alumina boat as the source material. Cleaned ITO substrates (area, 1 cm x 1 cm) were placed downstream of the precursor. The furnace was heated to a preset temperature and maintained at this temperature for 60 minutes. A mixture of Ar/O_2 as carrier gases, flowed into the quartz tube at a total flow rate of 60 SCCM to oxidize and transport the zinc vapor to the surface of substrates. Then, the system was cooled down naturally to ambient temperature.

Core-shell ZnO and ZnO/ZnSe synthesis

3.1 ZnO/ZnSe core-shell nanowire array by PLD method

In the past decade, pulsed laser deposition, PLD, is considered a very exciting technique that has been widely used and applied for a variety of materials. It has been extensively utilized to deposit or coat thin films for superconductors, semiconductors and insulators. The idea of this technique is based on the interaction of a pulsed laser beam with the surface of a solid target (31). The PLD of a semiconductor compound has been successfully carried out in our research group for optoelectronics and solar cell application with good optical properties (32) (33) and (34).

Thin films properties, such as crystalline structure, thickness, stoichiometry and composition, can be controlled by using pulsed laser deposition, PLD, technique. Moreover, excellent coating properties can be obtained through low deposition temperatures. However, PLD has a series of disadvantages, some examples of this are that roughness and clusters may appear at the surface resulting in bad optical and electrical properties. Additionally, it cannot be made into larger amounts (35).

Deposition parameters are extremely critical to the structural and optical properties of the deposited layer. For example, when we need to control the thickness of a shell, there are several important factors to consider, such as target-to-substrate distance, deposition duration, pulse repetition frequency, and laser energy density. Particularly, laser energy density fluence (F) which governs (i) the deposition rate, (ii) the number of particulates, and (iii) the stoichiometry and the uniformity of film thickness. Moreover, as the laser energy density increases, the thickness of the deposited layer will be increased in the central region. In addition, temperature can effectively manage structural, optical, and electrical properties of the zinc selenide thin layer (35) and (36). Therefore, it is very important to optimize such parameters to study the structural and optical properties of the as-synthesized ZnO/ZnSe core/shell nanowire array (37) and (38).

3.2 Structures analysis of ZnO/ZnSe core-shell nanowire

A two-step synthesis has been utilized to fabricate type II heterojunction ZnO/ZnSe core/shell nanowire array. First, as-grown ZnO NWs on ITO substrates (area, 1 cm x 1 cm), their samples were taken to be examined by Scanning Electron Microscope, SEM, to look for morphological and structural details of the as-synthesized ZnO. Subsequently, the ITO substrate with ZnO nanowire array was taken to perform a coating layer of ZnSe layer on the surface of NWs.

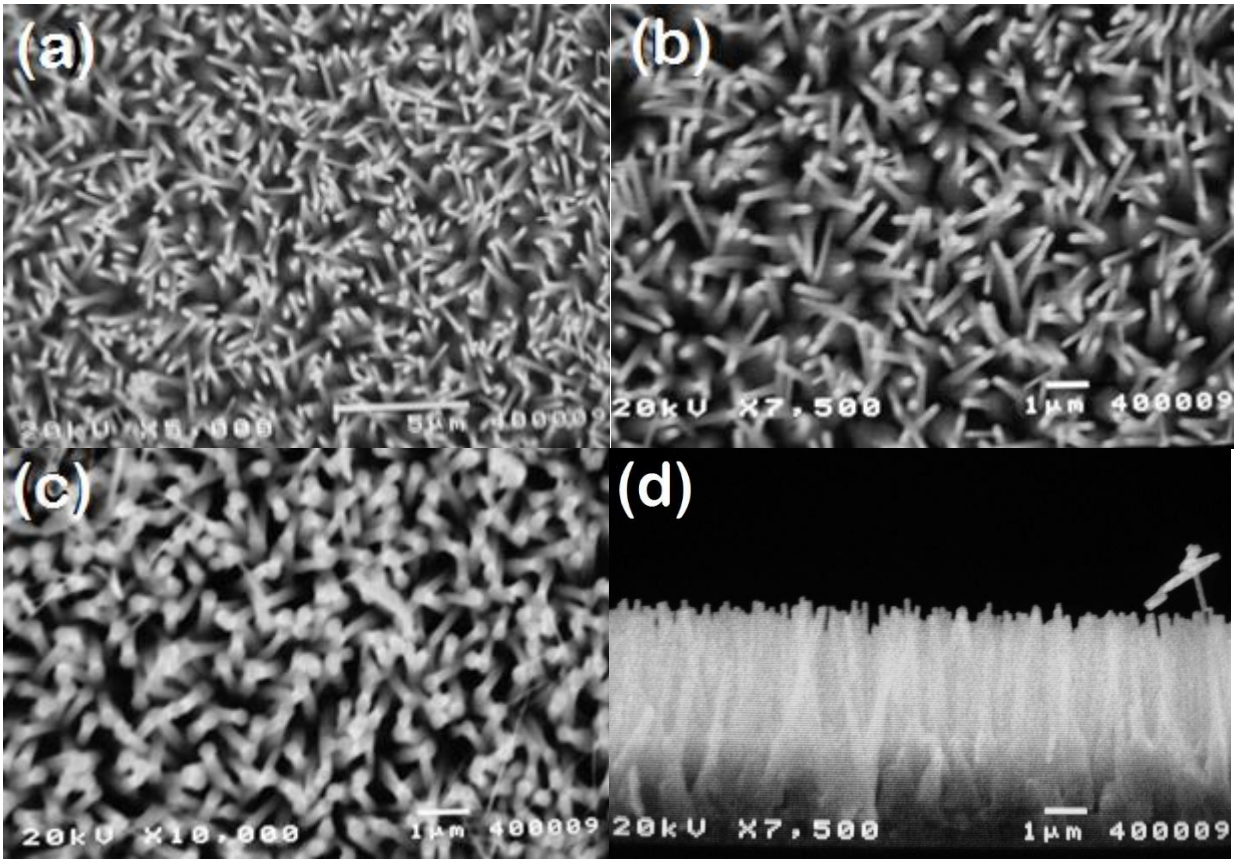

Figure 3.1 SEM images of ZnO nanowire array on ITO substrate (a, b and c) top-view SEM images at different magnifications of ZnO Nanowire array on ITO substrate (d) Cross-sectional SEM image of ZnO nanowire array with an average length of 5µm

The morphology of the as-synthesized ZnO nanowires were characterized using a JSM-5410 scanning electron microscope SEM. Figure 3.1 shows typical SEM images of the as-synthesized ZnO nanowires with smooth surfaces and high density. As shown in Figure 3.1(a), (b) and (c), top-view SEM images at lower and higher magnifications of the ZnO nanowires which were

synthesized by CVD method revealed that entire ITO substrate 1cm×1cm was covered with nanowire array and high density nanowires were obtained. A cross-sectional image in Fig. 3(d) exhibits the nanowires are perpendicular to the substrate and are varied in length. The SEM images indicate that ZnO nanowire arrays with high integrity have a diameter that is about 80–100 nm, while their length is about 5–8 micrometers. Therefore, ZnO nanowires are successfully grown on ITO substrates and ready to be processed for the next step.

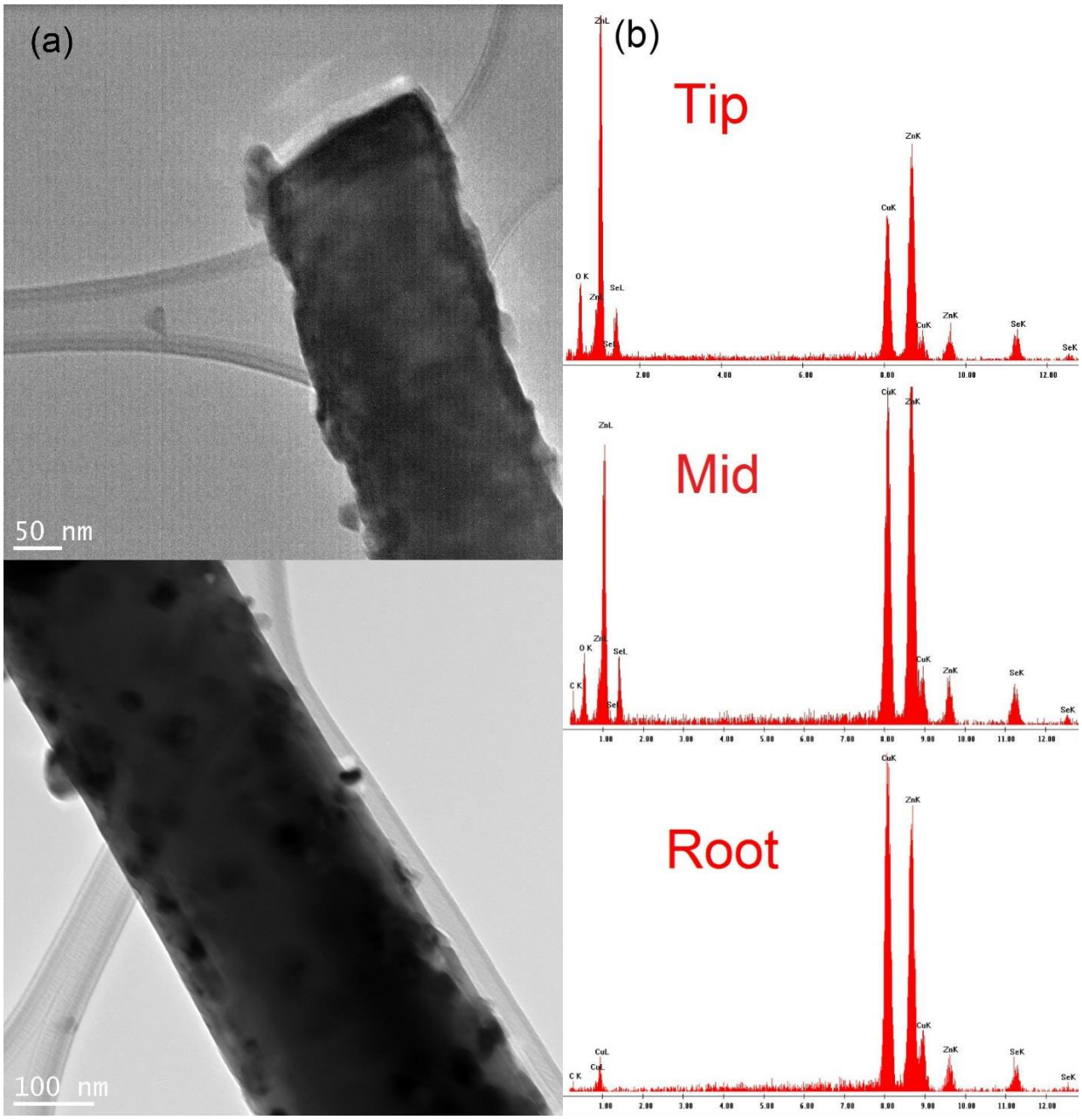

Figure 3.2 TEM image and EDX pattern of the as-synthesized ZnO/ZnSe core/shell heterostructures: (a) TEM image of the ZnO/ZnSe core/shell heterostructure tip upper and mid lower pictures. (b) The corresponding EDS spectrum of the samples taken from the NW tip, mid- and root, respectively. The signals for C and Cu peaks is originated from the amorphous carbon substrate and the TEM grid substrate, respectively.

In order to obtain detailed information of the as-synthesized ZnO/ZnSe core-shell nanowire Transmission Electron Microscope (TEM), JEOL Model 2010 with energy dispersive X-ray

spectrometer (EDS) was conducted to investigate the coated ZnO/ZnSe core/shell nanowire array structure. Figure 3.2(a) displays a typical low-magnification TEM image of a ZnO/ZnSe core/shell nanowire array heterostructures. The interface region between the ZnO core and ZnSe shell is clearly observed and the thickness of the ZnSe shell is about 18 nm. For further investigation, the corresponding EDS spectrum was conducted on tip middle and root of a single core/shell nanowire structure. Figure 3.2(b) shows the composition distribution of the as-synthesized ZnO/ZnSe core-shell nanowire array heterostructures, the spatial distribution of the ZnO and ZnSe elements in the core and shell, respectively, were obtained by using EDS spectrum. The spectrum exhibits strong Zn and Se peaks indicating the formation of ZnSe product. The C and Cu signals come from the amorphous carbon substrate and the TEM grid, respectively.

Device processing and measurements

4.1 Experimental

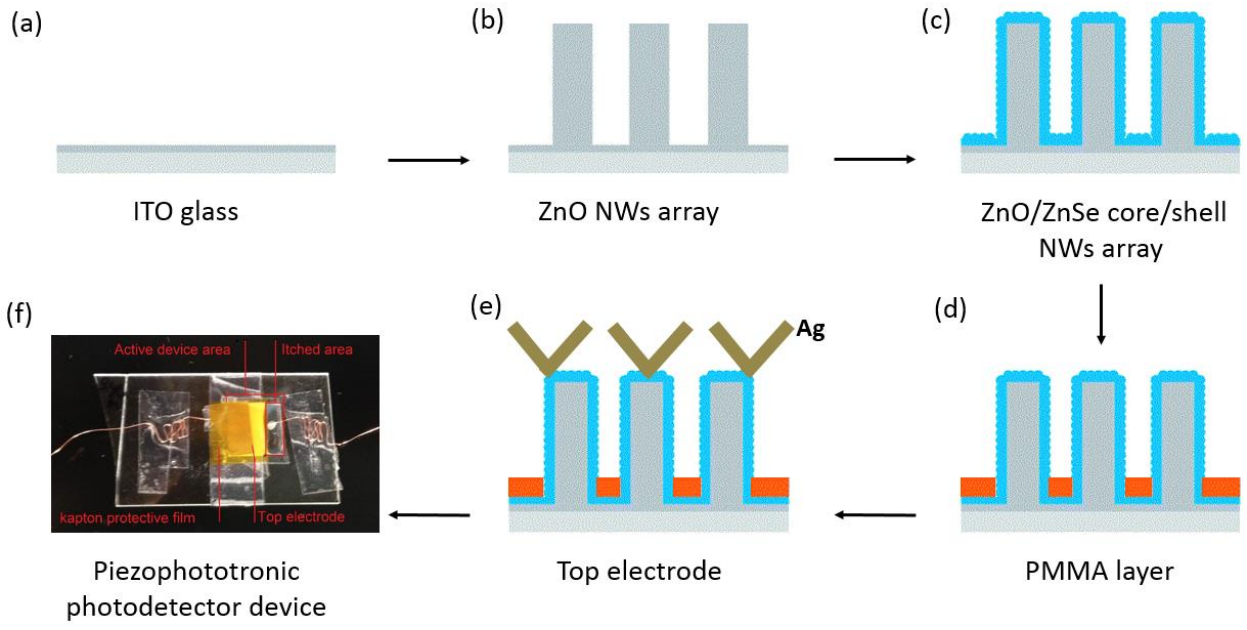

Figure 4.1 Schematic illustration of the fabrication process of ZnO/ZnSe core/shell NWs. A-F, present commonly used configurations of the device integration.

Figure 4.1 illustrates the brief fabrication of the final ZnO/ZnSe core/shell nanowire array heterostructures photodetector devices. After providing several procedures including: 4.1(a), ITO substrate with standard wafer cleaning procedure; 4.1(b), ZnO NWs grown on ITO sub. via CVD method; 4.1(c), ZnSe product as a shell coated on ZnO core using PLD technique; 4.1(d), PMMA layer spin-coated on ZnO/ZnSe core/shell; 4.1(e), Ag/polyester zigzag electrode on the tips of ZnO/ZnSe core/shell; 4.1(f), finished device structure where the device was integrated as followed. First, the portion of the ITO mother substrate was etched using diluted HCl so that a copper wire can be attached directly to the ITO surface. Second, after connecting a copper wire to the Ag/polyester zigzag using a silver paste, the top electrode was placed on the top of the ZnO/ZnSe and then kapton protective film was used to package the device.

Growth of ZnO nanowires NWs by Chemical Vapour Deposition (CVD)

The synthesis of ZnO nanowires was conducted on SiO_2 passivated indium tin oxide (ITO) coated glass substrate (R_s = 70 – 100 Ω) (area, 1 cm x 1 cm) via Chemical Vapour Deposition. ZnO NWs were initially synthesized on a cleaned ITO substrate to cover the entire substrate surface. The CVD system contained a horizontal quartz tube furnace with three heating zones, however only the central and right zones were used. Firstly, 4.0 g of high purity metallic Zn powder (Alfa Aesar, 99.9% purity, metals basis) as the source material was loaded into a ceramic boat and placed inside the chamber at the central heating zone. The target substrates were placed downstream of the Zn powder ceramic boat at the right zone. The target to the substrate distance was about 15 centimeters. Prior to heating, the system was pumped down to 1 x 10^{-3} Torr and filled with inert gases Ar/O_2. Argon and Oxygen gases with 40 and 300 SCCM flow rate, respectively, were introduced into the chamber to serve as the carrier gas. The reactor temperature was programmed via temperature controllers for the central and right zones as depicted in Figure 4.2. During the growing process, the right zone temperature ramped gradually at a rate of 10°C/min to 500°C and was maintained there for 150 minutes. The central zone temperature was kept for 50 minutes at room temperature and was raised slowly at a rate of 10°C/min to 900°C and held there for 60 minutes. After the tube was heated and the growth temperature reached the end, the chamber was slowly cooled to room temperature. Finally, The ZnO NWs with a diameter ranging from 80–100 nm were successfully grown on ITO substrates using chemical vapor deposition, CVD, method.

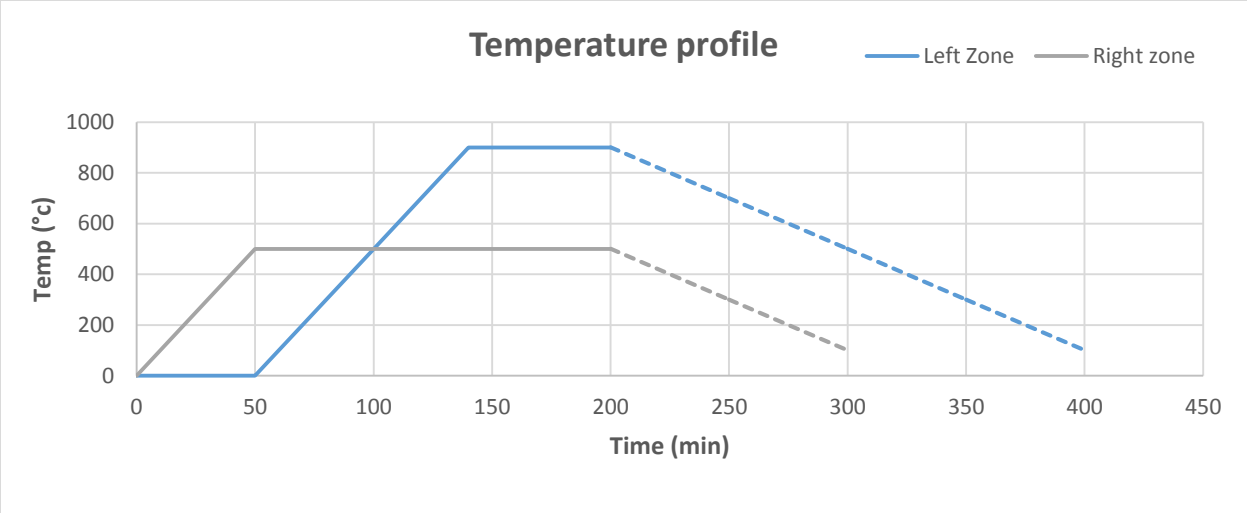

Figure 4.2. This graph shows the temperature profiles for both zones. The central heating zone is labeled as a blue line and the right heating zone as a grey line. The approximate time consumed for cooling each zone is depicted as dashed lines.

Deposition of ZnSe layer by pulsed laser deposition (PLD)

In order to synthesize ZnO/ZnSe core/shell nanowires, a single ITO substrate with as-grown ZnO nanowires was transferred into a pulsed laser deposition system. LOTIS TII LS-2147 Pulsed Nd:YAG Laser was applied to ablate the target. The laser wavelength, energy density, and pulse frequency were 1064 nm, 45 mJ cm^{-2}, and 3 Hz, respectively. The target substrate was loaded in a quartz tube and placed near the ZnSe target disc where the target source was cold-pressed into a pellet and placed into a ceramic boat. The quartz tube placed inside the furnace was first vacuumed 1 x 10^{-3} Torr base pressure one hour before raising the temperature. Then the temperature of the furnace was ramped gradually to 500 °C and left at this temperature during the deposition process, which lasted for 10 minutes. After the deposition process took place, the chamber was allowed to cool down naturally. Finally, the coating of ZnSe layer on the ZnO NWs surface was successfully carried out and the substrate was ready for structural, optical characterizations and device fabrication.

4.2 Piezo-phototronic photodetector performance of ZnO/ZnSe nanowire array

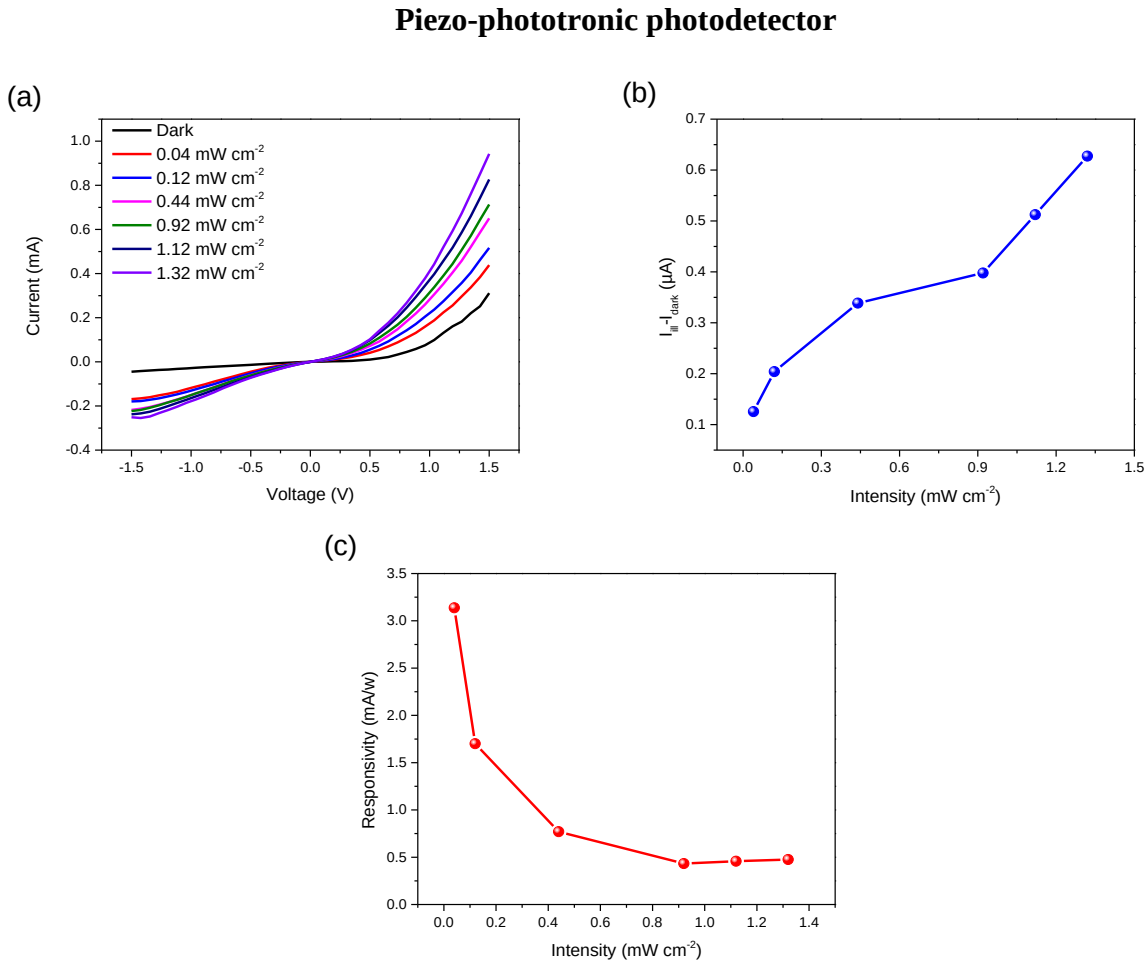

Figure 4.3 IV Current–voltage characteristic of ZnO/ZnSe core/shell nanowire array photodetectors under different UV illumination densities as shown in Figure (a). Photocurrent response under variable UV illumination (b) and (c) calculated relative responsivity under various illumination densities

To test the performance of the device, *I–V* measurement of the photodetector ZnO/ZnSe core/shell nanowire array integrated on ITO substrate were conducted. It is well known that electron–hole pair is created in type II heterostructures by a photon incident to semiconductors (17) and (20). First of all, an original *I–V* characteristic of the device was measured in a dark condition. Then a variety of UV light intensity of 0.04, 0.12, 0.44, 0.92, 1.12 and 1.32 mW cm^{-2} at a bias of 1.5 V were applied for all of the measurements. These experimental results in Figure 4.3(a) show that

the photocurrent increases when UV illumination density is increased, which means an increment of electron–hole pair rate occurs due to the effect of higher intensity. Figure 4.3(b) exhibits photocurrent versus illumination intensity plotting that was taken from Figure 4.3(a) where a pronounced increase in photocurrent curves appear in proportion to the light intensity. The responsivity (R_λ) at a particular wavelength was calculated and plotted as shown in Figure 4.3(c). The responsivity equation at a practical wavelength is described as follows (39)

$$R_\lambda = \frac{I_{light} - I_{dark}}{P_{ill}}$$

Where,

I_{light} = Current when the photodetector is under illumination

I_{dark} = Current when the photodetector is in the dark

P_{ill} = Excitation power

And light intensity (P_{ill}) can be calculated as

$$P_{ill} = I_{ill} \times A$$

Where,

I_{ill} = Illumination density

A = Active illuminated device area

These excellent specific electrical properties are due to using CVD technique to grow ZnO NWs and PLD method for coating NWs with ZnSe shell.

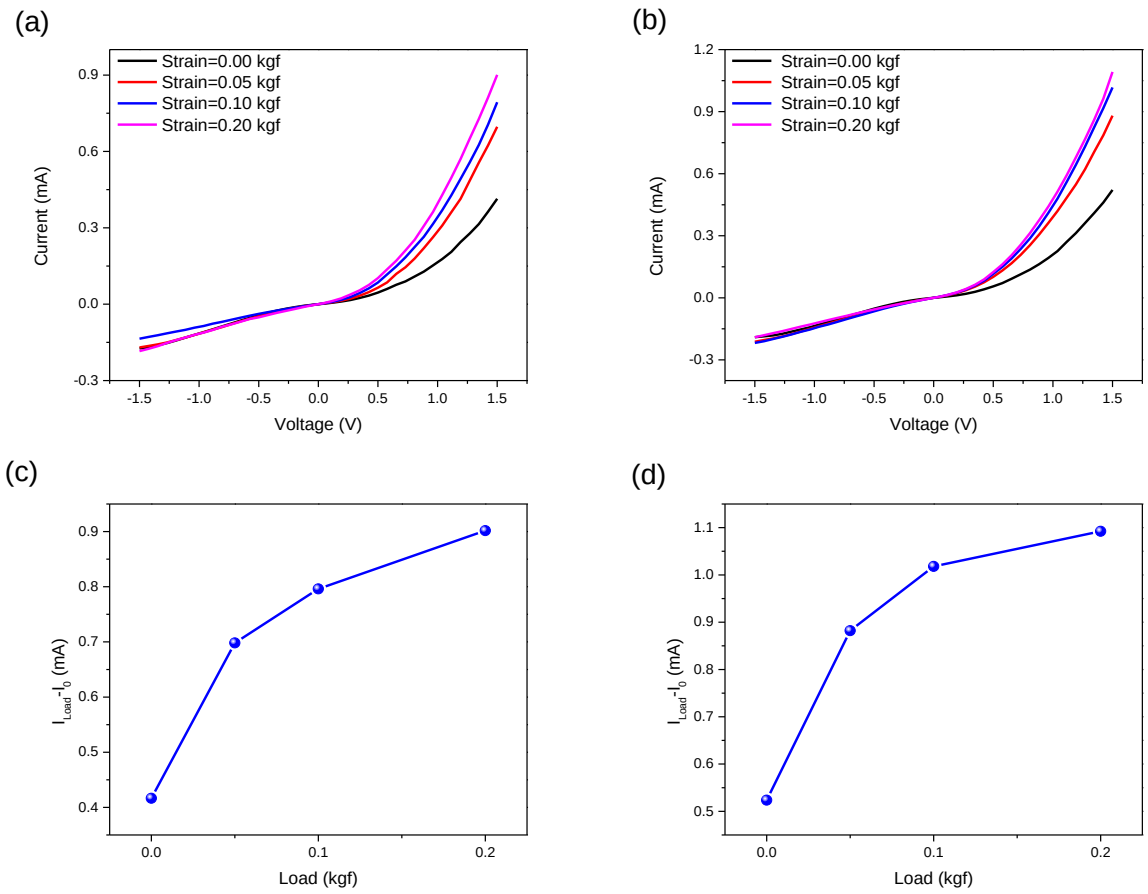

Figure 4.4 IV Current–voltage characteristic of ZnO/ZnSe core/shell nanowire array photodetectors under different compressive loads. As shown in (a) and (b), the photocurrent response under different compressive loads when the illumination density is 0.04 mW cm^{-2} and 0.12 mW $cm^{-2,}$ respectively. Figure (c) and (d) display photocurrent response with respect to compressive loads for (a) and (b), respectively.

To investigate the influence of the inherent piezopotential of ZnO/ZnSe core/shell nanowire array *I–V* measurements were done. ZnO/ZnSe core/shell nanowire array photodetector devices were measured with/without compressive loads and at ultraviolet UV illumination densities of 0.04 mW cm^{-2} and 0.12 mW cm^{-2} at a bias of 1.5 V, respectively. Figure 4.4(a) displays a variety of axial compressive loads on the nanowire from 0.05 kgf to 0.20 kgf (kilogram force) at a fixed wave length of 0.04 mW cm^{-2} where photocurrent peaks arise when a compressive load is being increased on the photodetector devices. Another *I–V* measurement with the same strains and only a change in light density to 0.12 mW cm^{-2} was performed in Figure 4.4(b). It gives similar results for the photocurrent increment in comparison to the pervious figure. However, the peak photocurrent 1.1 mA at 0.12 mW cm^{-2} is found to be higher than that of 0.04 mW cm^{-2} 0.9 mA,

which is reasonable. Additionally, the photocurrent peaks can be recovered as the compressive load was released. Figures 4.4(c) and 4.4(d) are the plotted result for the change in peak photocurrent versus compressive load for figures 4.4(a) and 4.4(b). The current mA for 0.04 mW cm^{-2} and 0.12 mW cm^{-2} illumination is significantly enhanced from 0.4 mA to 0.9 mA and from 0.5 mA to 1.1 mA, respectively, by introducing the compressive load, although the compressive load has little effect on the sensitivity to stronger light illumination. Therefore, the detection sensitivity of the nanowire-based photodetector is enhanced upon the UV light illumination when the ZnO NWs experiences compressive load.

Energy Band Diagram

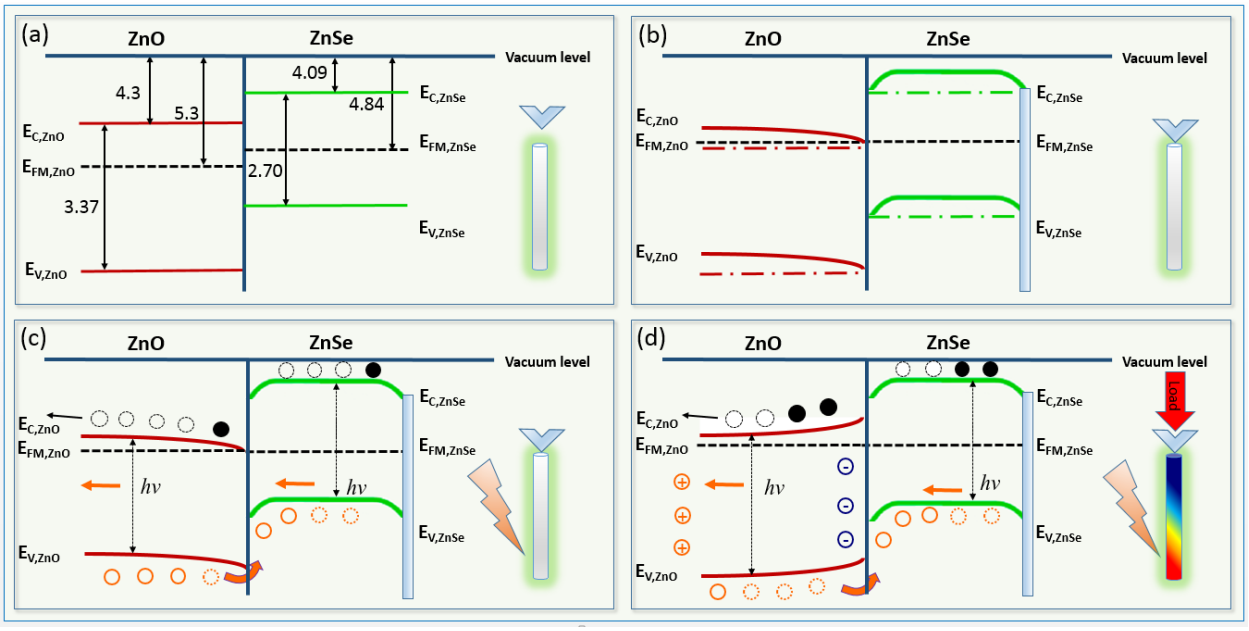

Figure 4.5 Schematic diagram displays type-II energy band alignment of ZnO/ZnSe heterojunction. The solid lines (green and red) in (a) show the natural band alignments, and the black dashed line shows Fermi level for both ZnO/ZnSe. (b) The dashed lines show the original conduction and valence band, respectively, and curved lines indicate the effective band gap position when the silver coated polyester zigzag electrode is being positioned on the top of nanowires array. (c) Under UV illumination only and (d) under applied load (32) & (37).

The energy band structure diagram of ZnO/ZnSe core/shell heterostructures is depicted in Fig. 4. In order to understand the piezo-phototronic enhanced performance of type-II heterostructures

ZnO/ZnSe core/shell nanowire array photodetector, a schematic band diagram has been drawn to show energy band realignment in different states. As shown in the diagram above, (a) natural band alignments, (b) sliver Ag zigzag on the top of core/shell structure, (c) under UV illumination only and (d) under compressive load and UV light. Figure 4.4(a) displays the type-II heterostructures band alignment of ZnO/ZnSe. When silver zigzag has not been attached, the Fermi level of ZnSe is higher than ZnO where the bandgap, electron affinities and work function for ZnO and ZnSe are equal to 3.37 eV, 2.7 eV, 4.3 eV, 4.09 eV, 5.3eV and 4.84eV, respectively. All values were taken from publications (10, 11 and 13). The vacuum level is defined as the energy of the electron at rest far from the influence of the potential of the solid and the work function is the energy required to take an electron from the Fermi level to the vacuum level, while the electron affinity of a semiconductor is the energy required to remove an electron from the bottom of the conduction band to the vacuum level (32) and (37).

In Figure 4.4(b), as the fermi level of ZnSe is higher, it means that there are more energy states in ZnSe than ZnO. Now, when Ag silver zigzags into contact, electronic flow will occur to balance the charge imbalance in the composite material. In other words, the shifting of energy bands continues until the energy levels $E_{FM,ZnO}$ and $E_{FM,ZnSe}$ are equalized. Therefore, after both $E_{FM,ZnO}$ and $E_{FM,ZnSe}$ have reached equilibrium energy or gotten to the same level, a downward bending of $E_{C,ZnSe}$ and $E_{V,ZnSe}$ took place. For a semiconductor, when an intense ultraviolet UV light excites band to band transitions, additional energy gaps can evolve within the original bands. Therefore, a weak type II transition occurred between $E_{C,ZnSe}$ and $E_{V,ZnSe}$ as shown in Figure 4.4(c) Upon straining and light illumination, upward bending of ZnO took places because of the negative piezoelectric charges were generated as displayed in Figure 4.4(d)

Conclusion

In summary, an enhanced photoresponse of type II ZnO/ZnSe heterostructures nanowire array with the ZnSe coated-NW-array as the shell and ZnO NW array as the core was developed. The photodetector displayed sensitive photoresponse to different light intensity 0.04, 0.12, 0.44, 0.92, 1.12 and 1.32 mW cm^{-2} with an external bias of 1.5 V. The excellent photoresponse of the photodetector device is due to the abrupt interface between ZnO and ZnSe. In addition, when compressive load was subjected to the photodetectors, the performance of the ZnO/ZnSe devices were further enhanced by order of magnitudes under UV illumination. This investigation demonstrates that the ZnO/ZnSe core/shell nanowires has a potential for photodetection with enhanced photoresponsivity.

REFERENCES

1- Kasap, S. O., & Capper, P. (2006). Springer handbook of electronic and photonic materials. New York: Springer

2- Cho, S., Jang, J., Lim, S., Kang, H., Rhee, S., Lee, J., & Lee, K. (2011). Solution-based fabrication of ZnO/ZnSe heterostructure nanowire arrays for solar energy conversion. Journal of Materials Chemistry, 21(44), 17816-17822.

3- Boxberg, F., Søndergaard, N. and Xu, H. Q., Photovoltaics with piezoelectric core-shell nanowires. AIP Conference Proceedings, (2011) 1399(1), 469-470.

4- Anderson, J, Chris G, V and de, W, Fundamentals of zinc oxide as a semiconductor. Reports on Progress in Physics. (2009) 72, 12, 126501.

5- Kołodziejczak-Radzimska, A. and Jesionowski, T. Zinc Oxide—From Synthesis to Application: A Review. *Materials* (2014), *7*, 2833-2881.

6- Bacaksiz, E., Parlak, M. and Tomakin, M. The effect of zinc nitrate, zinc acetate and zinc chloride precursors on investigation of structural and optical properties of ZnO thin films. J. Alloy. Compd. (2008), 466, 447–450.

7- N. Izyumskaya , V. Avrutin and Ü. Özgür, Preparation and properties of ZnO and devices, Phys. Status Solidi B (2007) 1439–1450

8- Alivov Ya. I., Liu C., Teke A. and Reshchikov M. A., A comprehensive review of ZnO materials and devices. J. Appl. Phys. (98), pp. 041301(103)

9- Tian, Wei, Hao Lu, and Liang Li, "Nanoscale ultraviolet photodetectors based on onedimensional metal oxide nanostructures. Nano Research. 8, 2, 382, (2015).

10- Takahashi, K., Sandhu, A., and Yoshikawa, A., Wide Bandgap Semiconductors: Fundamental Properties and Modern Photonic and Electronic Devices. Berlin, Heidelberg: Springer-Verlag Berlin Heidelberg, 2007.

11- Wang, ZL and Song, J., Piezoelectric Nanogenerators Based on Zinc Oxide Nanowire Arrays. Science. 5771, 242, 2006. ISSN: 00368075.

12- Ashraf M., Akhtar S. and Khan A., Effect of annealing on structural and optoelectronic properties of nanostructured ZnSe thin films. Journal of Alloys and Compounds, (2015) 2011; 509:2414-2419.

13- Venkatachalam S., Mangalaraj D. and Narayandass S., Structure, optical and electrical properties of ZnSe thin films. Phys. B: Physics of Condensed Matter (2005) 358:27-35.

14- Manbachi, A., and Cobbold, R. C., Development and application of piezoelectric materials for ultrasound generation and detection. Ultrasound, (2011) 11(4), 187-196.
15- Zhao W., Xumin P. and Yahua H.,Piezoelectric Nanowires in Energy Harvesting Applications, (2015) vol. 2015 pp 165631, 21
16- D.J. Jones, S.E. Prasad, J.B. Wallace, "Piezoelectric Materials and their Applications", Key Engineering Materials, (1996) Vols. 122-124, pp. 71-144
17- WANG, ZL. Review: Piezopotential gated nanowire devices: Piezotronics and piezo-phototronics. Nano Today. (2010) 5, 540-552.
18- Boxberg, F, Sondergaard, N and Xu, HQ. Elastic and piezoelectric properties of zincblende and wurtzite crystalline nanowire heterostructures. Advanced Materials (2012) 24: 4692–706.
19- M. Vos, F. Xu and J. H. Weaver, "Influence of metal interlayers on Schottky barrier formation for Au/ZnSe (100) and Al/ZnSe (100)," Applied Physics Letters, vol. 53, no. 16, pp. 1530–1532, 1988.
20- Liu Y., Zhang Y. and Yang Q., Fundamental theories of piezotronics and piezo-phototronics. Nano Energy. (2015) 2014.11.051.
21- Xiang Y. K. and Zhong L. W., Polar-surface dominated ZnO nanobelts and the electrostatic energy induced nanohelixes, nanosprings, and nanospirals. Applied Physics Letters. (2004) 84(6):975-977.
22- Zhong Lin Wang,Zinc oxide nanostructures: growth, properties and applications, J. Phys. Matter 16 (2004) R829–R858
23- J. Kobayashi, H. Sekiwa and M. Miyamoto, Crystal Growth & Design (2009) 9 (2), 1219-1224
24- A. Lopez-Otero: Thin Solid Films 49, 1 (1978)
25- Tak, Y. J.; Ryu, Y. H.; Yong, K. Nanotechnology (2005), 16, 1712
26- H. M. Manasevit, W. I. Simpson: J. Electrochem. Soc.118, 644 (1971)
27- Bjork, M. T. Ohlsson, B. J. Sass, T and Persson, A, Appl. Phys. Lett. (2002), 80, 1058.
28- T. Suntola: Mater. Sci. Rep. 4, 261 (1989)
29- Lyapina, O. A., Baranov, A. N. and Panin, G. N. Synthesis of ZnO nanotetrapods. Inorganic Materials (2008), 44(8), 846-852.

30- Anthony c. J. and michael l. H., Overview of Chemical Vapour Deposition, (2008) ISBN: 978-0-85404-465-8.

31- E. Morintale, C. Constantinescu and M. Dinescu, Thin films development by pulsed laser-assisted deposition, physics auc, (2010) vol. 20, 43-56

32- S. C. Rai, K. Wang and Y. Ding, Piezo-phototronic Effect Enhanced UV/Visible Photodetector. ACS Nano (2015) 9 (6), 6419-6427

33- Wang, K., Chen, J.and Zhou, W., Direct Growth of Highly Mismatched Type II ZnO/ZnSe Core/Shell Nanowire Arrays on Transparent Conducting Oxide Substrates for Solar Cell Applications. Advanced Materials, (2008) 20(17), 3248.

34- S. Wozny, K. Wang, and W. Zhou, Cu2ZnSnS4 nanoplate arrays synthesized by pulsed laser deposition with high catalytic activity as counter electrodes for dye-sensitized solar cell applications, Journal of Materials Chemistry A: Materials for Energy and Sustainability (2013), 1(48), 15517-15523.

35- Venkatachalam S., Mangalaraj D. and Narayandass S., Influence of substrate temperature on the structural, optical and electrical properties of zinc selenide (ZnSe) thin films. (2005) 39, 22, 4777-4782

36- Perna G., Capozzi V., and Plantamura M., Structural and optical properties of pulsed laser-deposited ZnSe films. Applied Surface Science, (2002) Volume 186, Issues 1–4 521-526.

37- Chen W., Zhang N. and Zhang M. Y., Controllable growth of ZnO-ZnSe heterostructures for visible-light photocatalysis, Cryst. Eng. Comm., (2014) vol. 16, no. 6, pp. 1201–1206.

38- J. H. Simmons and K. S. Potter, Optical Materials, Academic Press, N Y. (2001) 35, 131-133. ISSN: 0143-8166.

39- Liu, Y., Yang, Q. and Zhang, Y., Nanowire Piezo-phototronic Photodetector: Theory and Experimental Design. Adv. Mater. (2012), 24, 1410–1417.

VITA

Fahad Dhafer Alqarni was born in Tabuk, Saudi Arabia. In June 2011, he received a Bachelor of Science with a major in chemistry from the University of Tabuk, Tabuk, Saudi Arabia. In the fall of 2013, he entered the Graduate School of The University of New Orleans and joined the Dr. Weilie Zhou group at the Advanced Materials Research Institute (AMRI) in January 2014 to obtain his master's degree in chemistry.